NASA TECHNICAL MEMORANDUM

NASA TM X-52226

GPO PRIC... $ ______

CFSTI PRIC...(S) $ ______

Hard ... 2.00

Microf... 150

ff 653 July ...

NASA TM X-52226

N66 31229 (ACCESSION NUMBER) 44 (PAGES) TMX 52226 (NASA CR OR TMX OR AD NUMBER) (THRU) 1 (CODE) 32 (CATEGORY)

FACILITY FORM 602

APPLICATION OF A DOUBLE LINEAR DAMAGE RULE TO CUMULATIVE FATIGUE

by S. S. Manson, J. C. Freche, and C. R. Ensign
Lewis Research Center
Cleveland, Ohio

TECHNICAL PAPER presented at Symposium on Crack Propagation sponsored by the American Society for Testing and Materials
Atlantic City, New Jersey, June 26 - July 1, 1966

NATIONAL AERONAUTICS AND SPACE ADMINISTRATION · WASHINGTON, D.C. · 1966

APPLICATION OF A DOUBLE LINEAR DAMAGE RULE TO CUMULATIVE FATIGUE

by S. S. Manson, J. C. Freche, and C. R. Ensign

Lewis Research Center
Cleveland, Ohio

TECHNICAL PAPER presented at

Symposium on Crack Propagation
sponsored by the American Society for Testing and Materials
Atlantic City, New Jersey, June 26 - July 1, 1966

NATIONAL AERONAUTICS AND SPACE ADMINISTRATION

E-3558

APPLICATION OF A DOUBLE LINEAR DAMAGE RULE TO CUMULATIVE FATIGUE

by S. S. Manson, J. C. Freche, and C. R. Ensign

Lewis Research Center
National Aeronautics and Space Administration
Cleveland, Ohio

SYNOPSIS

The validity of a previously proposed method of predicting cumulative fatigue damage based upon the concept of a double linear damage rule is investigated. This method included simplified formulas for determining the crack initiation and propagation stages, and indicated that each of these stages could be represented by a linear damage rule. The present study provides a critical evaluation of the earlier proposal, further illuminates the principles underlying cumulative fatigue damage, and suggests a modification of the original proposal.

Data were obtained in two stress level tests with maraged 300 CVM, and SAE 4130 steels in rotating bending. Two strain level tests were conducted in axial reversed strain cycling with maraged 300 CVM steel. The investigation showed that in most cases the double linear damage rule when used in conjunction with originally proposed equations for determining crack initiation and propagation predicted fatigue life with greater or equal accuracy than the conventional linear damage rule. An alternate viewpoint of the double linear damage rule is suggested which may have value in the prediction of fatigue life under complex loading spectra. The results obtained to date are, however, limited, and the method must be regarded as tentative until further verification is obtained.

X-52226

INTRODUCTION

The subject of cumulative fatigue damage is extremely complex and various theories have been proposed (refs. 1 to 10) to predict fatigue life in advance of service. The most widely known and used procedure is the linear damage rule commonly referred to as the Miner (ref. 7) rule. It is well known that the linear damage rule, which indicates that a summation of cycle ratios is equal to unity, is not completely accurate; however, because of its simplicity and because it has been found to be in reasonable agreement with experimental data for certain cases it is almost always used in design. If a new method is to replace the linear damage rule in practical design it is important that much of the simplicity of the linear damage rule be retained. The double linear damage rule, considered herein, retains much of this simplicity and at the same time attempts to overcome some of the limitations inherent in the conventional linear rule.

One of the limitations of the linear damage rule is that it does not take into account the effect of order of loading. For example, in a two-stress level fatigue test in which the high load is followed by a low load, the cycle summation is less than unity, whereas a low load followed by a high load produces a cycle summation greater than unity. The effect of residual stress is also not properly accounted for by the conventional linear damage rule, nor does it take into account cycle ratios applied below the initial fatigue limit of the material. Since prior loading can reduce the fatigue limit, cycle ratios of stresses applied below the initial fatigue limit should be accounted for (ref. 10). In addition, "coaxing" effects present in some strain-aging materials (ref. 11) in which the appropriate sequence of loading may progressively raise the fatigue limit are not accounted for by the linear damage rule. Various methods have been proposed as alternatives to the linear damage rule. None overcomes all of the deficiencies and many introduce additional complexities which either preclude or make their use extremely difficult in practical design problems.

The possibility of improving the predictions of a linear damage rule by breaking it up into two phases, a linear damage rule for crack initiation and a linear damage rule for crack propagation, was first suggested by Grover in reference 12. No rational basis for this approach was indicated, nor were definite expressions provided for separating out the two phases. One of the authors of this paper considered these aspects in greater detail in reference 13. Total life was considered as consisting of two important phases, one for initiating a crack and one for propagating a crack, and a linear damage rule was applied to each of these phases. This double linear damage rule was intended to correct the deficiencies associated with order of loading; the other limitations cited above are not directly taken into account. Simplified formulas derived from limited data for determining the crack initiation and propagation stages were tentatively presented.

The present study was conducted to provide a critical evaluation of the proposal of reference 13, specifically the analytical expressions for separating out the two phases. Additional data were obtained in two stress level tests in rotating bending and two strain level tests in axial reversed strain cycling. The materials investigated were maraged 300 CVM and SAE 4130 steels. Fatigue life predictions by the double linear damage rule and the conventional linear damage rule are compared with experimental data. In addition, instead of using the analytical expression given in reference 13 to represent the crack propagation stage in the application of the double linear damage rule as originally proposed, a more generalized expression is suggested which involves the separation of the fatigue process into two experimentally determined phases. These are not necessarily the physical processes of crack initiation and propagation.

CONCEPT OF THE DOUBLE LINEAR DAMAGE RULE

Analytical Application

In reference 13 it was proposed that the crack propagation period $(\Delta N)_f$ and crack initiation N_o can both be expressed in terms of total fatigue life N_f by the following equations

$$(\Delta N)_f = PN_f^{0.6} \tag{1}$$

and

$$N_o = N_f - (\Delta N)_f = N_f - PN_f^{0.6} \tag{2}$$

where the coefficient $P = 14$. The experimental basis for the selection of this value of coefficient is given in references 13 and 14 and will also be further described later in the text. The equations expressing cumulative fatigue damage in terms of the double linear damage rule as proposed in reference 13 are:

For the crack initiation phase

$$\sum \frac{n}{N_o} = 1 \tag{3}$$

where $N_f > 730$ cycles, $N_o = N_f - 14\ N_f^{0.6}$

where $N_f < 730$ cycles, $N_o \approx 0$

If any part of the loading spectrum includes a condition where $N_f < 730$ cycles, an effective crack is presumed to initiate upon application of that first loading cycle.

For the crack propagation phase, the expression is

$$\sum \frac{n}{(\Delta N)_f} = 1 \tag{4}$$

when $N_f > 730$ cycles, $(\Delta N)_f = 14\ N_f^{0.6}$

when $N_f < 730$ cycles, $(\Delta N)_f = N_f$

where

N_o = cyclic life to initiate an effective crack at a particular strain or stress level

$(\Delta N)_f$ = cyclic life to propagate a crack from initiation to failure at a particular strain or stress level

N_f = cyclic life to failure of specimen

n = number of cycles applied at a particular strain or stress level

An example of the manner of applying these equations for a simple two stress level loading case is given in appendix A. Further discussion of the equation relating crack initiation and propagation to total fatigue life is presented in reference 14. It should be emphasized that these equations were derived on the basis of data obtained with 1/4 inch diameter specimens of notch ductile materials and have thus far been shown to be valid only for this size specimen (ref. 14). Of course, most materials would be notch ductile for such a small specimen size. This aspect is discussed more fully in reference 13.

By comparison the conventional linear damage rule is expressed as

$$\sum \frac{n}{N_f} = 1 \tag{5}$$

Equation (5) states that a single summation of cycle ratios applied at different stress or strain levels is equal to unity.

Graphical Representation of Double Linear Damage Rule

Applied to Two Stress Level Fatigue Test

Figure 1 illustrates the graphical representation of the double linear damage rule plotted in terms of the remaining cycle ratios, $n_2/N_{f,2}$, at a second stress level against the cycle ratios, $n_1/N_{f,1}$, applied at an initial stress level. Also shown is a dashed 45^{o} line which represents the conventional linear damage rule. The figure is illustrative of the case in which the prestress condition is the high stress and this is followed by operation to failure at a lower stress. The position of lines AB and BC would be located on the other side of the 45^{o} line for the condition of low prestress followed by operation to failure at a high stress. Referring to figure 1, according to the double linear damage rule, if the cycle ratios applied $(n_1/N_{f,1})$ are less than the number required to initiate an effective crack at a particular stress level, then the remaining predicted cyclic life ratio $(n_2/N_{f,2})$ would lie along AB. The linearity of AB is implicit in the assumption of a linear damage rule for crack initiation. Point B represents the cycle ratio applied at the first stress level which is sufficient to initiate an effective crack, so that upon changing to the second stress level the remaining cycle ratio at that stress level is exactly equal to the total propagation stage. The coordinates of this point are designated as $N_{o,1}/N_{f,1}$, and $\Delta N_2/N_{f,2}$. Beyond this initial cycle ratio $N_{o,1}/N_{f,1}$, the first applied cycle ratio is more than that required to initiate an effective crack, and the crack propagation phase is entered. This is represented by the line BC which is also straight reflecting the second assumed linear relation. The remaining cyclic life ratio then lies along line BC. Thus, in two-step tests in which a single stress level was applied for a given cycle ratio and the remainder of the life taken up at a second stress level, two straight lines positioned as shown would be expected. It should also be emphasized that point B is significant since it permits determination of both the effective crack initiation and propagation periods for both stress levels used in the test.

A final point should be made with respect to the graphical application of the double linear damage rule. Since lines AB and BC are straight and since points A and C are fixed, ideally only two tests are required to establish the positions of these lines and consequently the point B. The only requirement for selecting these tests is that in one test the cycle ratio applied at the initial stress level should be relatively large, and for the other test it should be relatively small, in order to insure that the remaining cycle ratios $n_2/N_{f,2}$ do not both fall on the same straight line, either AB or BC. The significance of obtaining point B in this simple fashion is apparent in the illustrative examples of appendices B and C.

EXPERIMENTAL PROCEDURE

Materials

Two steels, SAE 4130 and maraged 300 CVM were investigated. Their compositions, heat treatments and hardnesses are listed in table I and their tensile properties in table II. Two different types of test specimens were used to accommodate the R. R. Moore and Krouse rotating bending test machines. A third type of specimen was used for axial strain cycling tests. All three specimen types are shown in figure 2. The 4130 steel test specimens were machined after heat treatment. The maraged 300 CVM specimens were machined prior to aging and after aging, finish ground to remove the final 0.015 inch from the test section. In addition all rotating bending specimens were machine polished with abrasive cloth of three grit sizes (320, 400, and 500). After final polishing the specimens were subjected to a microscopic examination at 20X.

Tests

Specimens were subjected to rotating bending in modified R. R. Moore and Krouse rotating beam fatigue machines and to axial reversed strain cycling in hydraulically actuated axial fatigue machines. In the rotating bending tests a rotational speed of 5000 rpm was employed at the lower stress levels. In order to avoid the detrimental effect of severe heat accumulation due to hysteresis, rotational speeds as low as 100 rpm were employed at the higher stresses, and jets of cooling air were directed at the specimens. A specimen runout no greater than 0.001 inch full indicator reading was permitted upon installation into the fatigue machines. Additional details regarding the rotating bending test procedure are given in refs. 9 and 10. Axial fatigue tests were run at 20 cycles per minute. Details of the test procedure are given in reference 15.

The fatigue curves for each material were obtained by fairing the best visual fit curves through the median data points obtained at each stress or strain range level. The number of data points at each level varied from a maximum of 25 to a minimum of 2. In conducting the investigation specimens were prestressed at a single stress (in rotating bending tests) to the desired percentage of material life as determined from the fatigue curves of the original material and to a single strain range (axial fatigue tests) as determined from strain range-life curves of the original material. The specimens were then run to failure at various stress (or strain range) levels. The specific conditions are indicated on the figures that describe the results of these tests.

RESULTS AND DISCUSSION

Comparison of Experimental and Predicted Fatigue Life by Originally Proposed Double Linear Damage Rule and Conventional Linear Damage Rule

Figure 3 shows the results reported previously in reference 13 for maraged 300 CVM steel which were obtained from rotating bending tests. The stress levels were so chosen that life at the initial stress was approximately 1000 cycles and at the second stress 500,000 cycles. Experimental data are shown by the circles. The solid lines represent predicted behavior by the double linear damage rule using different values of the coefficient in equation (1). For a value of coefficient equal to 14 the predicted behavior was represented by the line ABG; for a coefficient of 12 it was ACG, etc. If a linear damage rule applied for the total life values, the behavior would be that shown by the dashed line AG. A reasonable agreement with the experimental data was obtained for a coefficient of 14. Since these data represent only one material and one combination of high and low stress equation (1) was only tentatively proposed (ref. 13) as being representative of cumulative fatigue damage behavior.

In extending this approach many additional tests were conducted with the same and with other materials in rotating bending and axial reversed strain cycling. Figure 4 shows the fatigue curves of these materials, maraged 300 CVM, and SAE 4130 steel, hard and soft. Since both Krouse and R. R. Moore machines were used for the 300 CVM tests the fatigue curves obtained with each machine are shown (fig. 4(a)). The curves are largely coincident. Figure 4(b) shows the fatigue curve for maraged 300 CVM steel obtained in axial reversed strain cycling.

Predictions of fatigue behavior by the double linear damage rule (using the expression $14\ N_f^{0.6}$ as representing the crack propagation stage) and the conventional linear damage rule are compared with experimental data in figures 5 and 6. Different combinations of loading corresponding to different life levels were chosen. Figure 5(a) presents the results from rotating bending tests for maraged 300 CVM steel designed to give relatively low fatigue lives of 1280, 1870, 2050, and 2350 cycles at the initial stress level. The loads at the second stress level were chosen to give lives up to 940 000 cycles. Generally the greater the difference between the initial and final life level (i.e., initial and final stress applied) the greater the deviation between the experimental data and the predicted behavior by the conventional linear damage rule shown by the 45° dashed line; also, the steeper is the first (corresponding to line AB, fig. 1) of the two solid lines which predict fatigue behavior by the double linear damage rule. Agreement between predicted fatigue behavior by the double linear damage rule and experimental data is good for these test conditions. This might be expected since the higher stress level as well as some of the lower stress levels are generally of the same order as those selected originally for determining equation (1) for this same material in reference 13.

Figure 5(b) deals with the same material but considers other combinations of test conditions in which the initial life level is relatively high. It is apparent that the greatest discrepancies between experimental data and predicted fatigue behavior by the double linear damage rule as originally proposed occur when both the initial and final life levels are high. It would be expected that this double linear damage rule would predict almost the same fatigue behavior as the conventional linear damage rule in these cases because the crack propagation period as determined from equation (1) would be relatively small. This is readily seen by using equation (1) for values of $N_{f,1}$ of 15 925, 47 625, 44 000, etc., the specific conditions which are considered in figure 5(b). The experimental data show appreciably lower values of remaining cycle ratio, $n_2/N_{f,2}$, than would be expected by either rule.

Figure 5(c) illustrates the results obtained under conditions of axial strain cycling with maraged 300 CVM steel. The initial life level was chosen in all cases to be less than 730 cycles. For this case the major part of the fatigue life would be taken up by the crack propagation period according to the expressions thus far assumed for crack propagation and initiation in applying the double linear damage rule. Since there is essentially no crack initiation stage, the predictions by the double linear damage rule should coincide with those by the conventional linear damage rule. This was the case for the two conditions in which the final stress level was chosen so as to give a low value of life $N_{f,2}$ and the experimental data agreed well with the predictions. However, when the second stress level was chosen so as to give a long life, $N_{f,2}$ = 15 950 cycles, the predicted fatigue life by the double linear damage rule was less than that obtained experimentally. It is apparent from figures 5(b) and (c) that there are deviations of the experimental data on both sides of the predictions made by the double linear damage rule when the expression $14\ N_f^{0.6}$ was used to represent the crack propagation stage.

Thus far consideration has been given only to the general case in which the high stress or strain (for strain cycling tests) was applied first. Figure 5(d) illustrates the opposite case. Except for the single axial strain cycling test the predictions by the double linear damage rule show general agreement with the experimental data. Regardless of deviations of individual data points from the predictions, however, it is evident from the figure that the order effect of loading is accounted for by the double linear damage rule.

The results for SAE 4130 steel are shown in figure 6. Part (a) of the figure deals with tests in which the initial life level was low and loads at the second stress level were chosen to give various life values up to 203 000 cycles. Part (b) of the figure considers cases where the initial life level was relatively high. In both cases, however, the order of load application was that of high stress followed by low stress. In general the results obtained with 4130 steel are the same as those obtained with the maraged 300 CVM steel for similar test conditions. For the most part agreement between predictions by the double linear rule using $(\Delta N)_f = 14\ N_f^{0.6}$ and experimental data was good, although deviations between predictions and data are clearly present in some cases. As was the case for the maraged 300 CVM steel, a more conservative prediction was always provided by the double linear damage rule, assuming the expression $14\ N_f^{0.6}$ as being representative of the crack propagation stage, than by the conventional linear damage rule when the high stress was applied first.

Examination of the Assumed Relation for Crack Propagation $(\Delta N)_f$

In view of the deviations noted between predictions and experimental results closer examination of the assumption that the crack propagation period $(\Delta N)_f$ may be expressed by the relation $14\ N_f^{0.6}$ is clearly in order. However, before considering the possibility of improving this relation by changing the coefficient or exponent or both, attempts were made to determine experimentally if the propagation period $(\Delta N)_f$ was indeed uniquely dependent upon fatigue life to specimen failure, N_f. The results of one such investigation are shown in figure 7. Values of ΔN_1 and ΔN_2 were obtained from two stress level tests with SAE 4130 soft steel in which $N_{f,1}$ was 485 cycles and $N_{f,2}$ was 14 000 cycles using the graphical method previously described and illustrated in figure 1. These values are plotted on figure 7 as points B and A'. The values of ΔN_1 and ΔN_2 similarly obtained from another set of data in which the $N_{f,1}$ was 14 000 cycles and $N_{f,2}$ was 203 000 cycles, are also plotted on figure 7 as points A and C. Obviously, points A' and A do not coincide as they would be expected to if

ΔN were solely a function of N_f. Thus, whether a given stress (corresponding to a fixed life) is used as the first or the second stress in a two stress level fatigue test is clearly significant and entirely different results can be obtained. If the representation of the crack propagation period by the expression $14N_f^{0.6}$ were correct the points determined as above would fall on the line with a slope of 0.6 when N_f values were greater than 730 cycles. It must therefore be concluded that the concept of representing crack propagation by a universal relation in terms of N_f, whether the coefficient is 14 or any other number, would produce some discrepancies. Other tests of the same type for other combinations of stress were also made. These gave similar results to those shown in figure 7.

There are probably several reasons why the crack propagation period is not uniquely related to total fatigue life (i.e., life to failure of the specimen). Reexamination is in order of the concept that the effective crack length for crack initiation is the same at all stress levels, and that extending a crack at a stress level different from that at which it was initiated is simply a continuation of the same process. Obviously the mechanisms involved are not as readily explainable. What may correspond to a crack length for effective crack initiation at one stress level may not be so at another stress level.

Another reason for the discrepancies relates to the hardening and softening characteristics of materials. Upon changing to a new strain level in a two step test, a material that hardens or softens extensively will not reach the same stress level for a given applied strain as it would have, had that same strain been maintained throughout the test. This is illustrated in figures 8 and 9. Figure 8 shows the stress response in axial strain cycling at constant strain amplitude for maraged 300 CVM steel. Two tests were run at each of two values of total strain. These were chosen to give lives on the order of 400 and 16 000 cycles. Agreement between the two tests run at each condition was good and demonstrated the ability to maintain and control approximately the same strain level on the fatigue machines used. Figure 9 illustrates the stress response in axial strain cycling two-strain level tests for maraged 300 CVM when the higher of these two strain levels was applied first and the lower strain level subsequently applied. It is evident that maraged 300 CVM is a strain-softening material. As continually increasing percentages of the life were applied at the higher strain level, the stress required to maintain that strain level progressively decreased. Also shown on the figure are the results of running for 5, 25, and 75 percent of the total life at the initial strain followed in each case by operation to failure at the lower strain level. In each case the stress required to maintain the lower level of constant strain in these two-step tests was lower than that required to maintain this level of strain in a single strain level test. Thus, the material was oversoftened as a result of the initial application of a high strain level. As a consequence one would expect a longer life than would be predicted by the double linear damage rule using the expression $14\ N_f^{0.6}$ as representing the crack propagation stage. Figure 9 shows this to be true. The circles represent the predicted lives according to the double linear damage rule using $(\Delta N)_f = 14\ N_f^{0.6}$; the crosses are the experimentally determined lives.

In order to describe the cumulative fatigue damage process more accurately methods must be sought to account for the factors discussed. This can be done while still retaining the double linear damage rule concept as discussed in the next section.

An Alternate Viewpoint of the Double Linear Damage Rule

In the suggested alternate approach the concept of crack initiation and propagation in the literal sense is altered to represent two effective phases of the fatigue process which might be designated as Phases I and II. The assumption of a linear damage rule for each of these two phases, however, would be retained. That such an assumption is reasonable may be seen by inspection of the data obtained in this investigation. This is particularly evident from some of the rotating bending test results obtained with SAE 4130 steel shown in figure 6(a). These results are replotted in figure 10 to illustrate how well two straight lines originating at ordinate and abscissa values of 1.0 fit the data. The coordinates of the intersection of these lines (as defined in fig. 1) determine the values of N_0 and ΔN used to establish the fatigue curves which represent phase I and phase II of the fatigue process. In keeping with this change in concept the form of the rule would be different for different materials and for different extreme loads that might be applied in a test. Additional experimental verification of this approach is still needed; however, it would seem to take into account the complexities discussed in an approximate fashion. It is interesting to note that the use of a new fatigue curve different from that of the original material in predicting remaining fatigue life after prestressing is not inconsistent with other methods such as that of Corten and Dolan (ref. 4). In general such previous approaches have assumed that the modified fatigue curves are best determined from a consideration of the highest and lowest stress levels of the applied spectrum. This basic approach will also be adopted in the following treatment.

To apply the double linear damage rule in the light of this revised concept to any anticipated loading spectrum for a given material a decision must first be made as to which are the highest and lowest loads of importance. Stress levels below the fatigue limit will not be considered for the present. A series of two stress level tests would be run in which the highest stress level would be applied first followed by operation to failure at the lowest stress level of significance within the loading spectrum. This should bring into play the important variables such as any extremes of hardening or softening of the material and extremes of crack length involved in initiating the propagating an effective crack. From such a series of tests it is possible to determine for that particular combination of stress levels the values of N_o and ΔN for both stresses by using the graphical procedure for applying the double linear damage rule as previously described. These values may then be plotted as shown in figure 11 at the two stress levels and curves sketched between these points that are consistent with the appearance of the original fatigue curve. It would then be possible to analyze the effect of block or spectrum loading of any pattern that could also include loadings between the highest and lowest levels by the double linear damage rule. The N_o and ΔN curves would be used for determing the effective values of phase I and phase II of the fatigue process. These curves would replace the expression $(\Delta N)_f = 14\ N_f^{0.6}$ or any other variation of such a formula. One example of applying this procedure is given in Appendix B.

Although at this early stage of the development of this approach, it seems most convenient to use a two-level test as illustrated in figure 1 to determine the effective values of Phases I and II for given extremes of stress or strain level within a given loading spectrum, further consideration may reveal better approaches for particular circumstances. For example, it may be desirable to use a block loading in which the highest and lowest significant stresses in the cycle are more typical of the spectrum of service loading for establishing the point of effective transition between the two phases (Point B in fig. 1), rather than merely following the high stress cycles by continuous loading at the lower stress. Since only two unknowns are involved (the points of effective transition from Phase I to Phase II for each of the two stress levels when applied in conjunction with the other) only two tests would be required to determine the two unknowns. This approach is further discussed in the Concluding Remarks.

Limited Experimental Verification of Alternate Viewpoint of Double Linear Damage Rule

In order to provide an indication of the validity of the alternate viewpoint of the double linear damage rule, a series of repetitive alternating two stress level block tests was conducted. Such a test may be considered as the next step in complexity to the single block two stress level test which provided the bulk of the data obtained in this investigation. The manner of conducting the test is fully described in Appendix C. Briefly, a two stress level single block base was selected. Equal fractional portions of the number of cycles at each stress level in the block were applied in a repetitive fashion. The double linear damage rule was applied to predict the summation of the cycle ratios required to cause failure using experimentally determined curves representing phase I and phase II of the fatigue process. A numerical example illustrating the use of this method in making these predictions is also given in Appendix C.

The experimental results of these tests as well as the predictions are shown in figure 12. The summations of the cycle ratios are plotted against the fractions of the basic block considered. Part (a) of the figure deals with the summation of cycle ratios applied at the high stress; part (b) with the summation of cycle ratios at the low stress; and part (c) with the total summation. The experimental data shown represent the arithmetic averages of 3 data points obtained at each fraction of the block considered. In general, there is reasonable agreement between the predicted results and the experimental data. The irregularity in the predicted results is probably associated with failure in either the high or low portions of the block loading pattern. In all cases the predictions by the double linear damage rule are conservative. Of course, it is important to note that much additional experimental verification is needed to fully establish the usefulness of the double linear damage rule in predicting remaining fatigue life for more complex loading spectra. The single series of tests contained in figure 12 serve more to illustrate the approach than to prove validity of the method.

CONCLUDING REMARKS

It should be emphasized that the conclusions drawn are based upon only a partially completed study of the problem of cumulative damage. However, it can be concluded that while a double linear damage rule involving the assumption that $(\Delta N)_f = 14\ N_f^{0.6}$ gives better results than the conventional linear damage rule it is not adequate where crack initiation and propagation are expressed solely in terms of total life. Other representations of crack initiation and propagation might be more accurate, but they must in some way take into account the hardening and softening characteristics of the material and more particularly the effect of the stress levels involved. An alternate viewpoint of the double linear damage rule in which the concept of crack initiation and propagation in the literal sense is altered to represent two effective phases of the fatigue process designated as phases I and II which can be determined experimentally, appears to overcome some of the limitations of the original proposal. The form of the rule then becomes different for different materials and for different extreme loads that might be applied in a test. It is conceivable that the double linear damage rule when applied in this manner might be more applicable to the study of complex structures.

More research is needed, however, to determine the validity of the approach and to establish the most effective manner of determining the point of transition between the two phases of the two extremes of the stress levels involved in the test. For example the type of block loading used as an illustration in Appendix C and figure 12 might in fact be used for the determination of the transition from phase I to phase II for each of the stress levels involved. The calculation need only be inverted to determine this transition for each of the two stress levels by the use of the two linear damage rules, the computations being similar to those shown in Appendix C. In this manner it may be possible to use a more realistic apportionment of the two stress levels to represent more closely their occurrence in the particular service histroy involved. Even more complex loadings simulating service loading could be envisioned, but these have not been pursued in view of the preliminary nature of this program. However, it is significant to recognize that the concept involved in the use of a double linear damage rule lends itself to further refinements. These could make the method more realistic with respect to the type of service for which life estimates would be made.

APPENDIX A. - APPLICATION OF DOUBLE LINEAR DAMAGE RULE TO A TWO STRESS LEVEL TEST USING THE RELATION $14\ N_f^{0.6}$ TO DEFINE THE CRACK PROGATION PERIOD

Given two stress levels 1 and 2, at which total life of the original material is $N_{f,1}$ and $N_{f,2}$ respectively, and a prestress cycle ratio $n_1/N_{f,1}$; it is desired to find the number of cycles that can be applied at the second stress level. The values of ΔN_1 and ΔN_2 are first determined from equation (1). The values of $N_{o,1}$ and $N_{o,2}$ can then be obtained by subtraction using equation (2). Next, determine the ratio $N_{o,1}/N_{f,1}$. For the case where $N_{f,1} > 730$ cycles, if $n_1/N_{f,1}$ is equal to $N_{o,1}/N_{f,1}$, the crack initiation stage has just been completed and the cyclic life remaining at the second stress level is exactly equal to that making up the crack propagation period, or

$$n_2 = N_{f,2} - N_{o,2} = \Delta N_2 \tag{1A}$$

If the ratio $n_1/N_{f,1} > N_{o,1}/N_{f,1}$, the life remaining at the second stress level may be expressed as

$$n_2 = \left[1 - \frac{\left(n_1 - N_{o,1}\right)}{\Delta N_1}\right] \Delta N_2 \tag{2A}$$

If the ratio $n_1/N_{f,1} < N_{o,1}/N_{f,1}$, the life remaining at the second stress level may be expressed as

$$n_2 = \left(1 - \frac{n_1}{N_{o,1}}\right) N_{o,2} + \Delta N_2 \tag{3A}$$

For the case where $N_{f,1} < 730$ cycles it is assumed that there is no lengthy crack initiation period, but rather that total life consists only of crack propagation. Then the life remaining at the second stress level can be determined from the expression

$$n_2 = \left(1 - \frac{n_1}{N_{f,1}}\right) \Delta N_2 \tag{4A}$$

In effect then for the latter case total life at stress 2 is determined from the linear damage rule for crack propagation only.

APPENDIX B. - APPLICATION OF DOUBLE LINEAR DAMAGE RULE USING EXPERIMENTAL DATA TO DEFINE PHASES I AND II OF FATIGUE PROCESS

In this appendix detailed examples will be given to show how the phase I and phase II curves of figure 11 were obtained and how these curves might possibly be used to predict the life of a three stress level fatigue test.

To define the two phases of the fatigue process some 2 stress level tests must first be conducted using the highest and lowest stresses of importance in the particular loading spectrum under consideration. For purposes of this illustration the material chosen was maraged 300 CVM steel and the two stresses chosen were 290 000 psi and 120 000 psi. From the original fatigue curve of figure 11 for this material (obtained on a Krouse machine) $N_{f,1}$ and $N_{f,2}$ equal 1280 and 244 000 cycles respectively. The data obtained from a series of tests conducted by applying various cycle ratios $n_1/N_{f,1}$ at the high stress and operating to failure at the low stress, are plotted in figure 13. Straight lines were then fitted through the data. These were required to originate from cycle ratio values of 1.0 on the ordinate and abscissa. The coordinates of the intersection point B are $n_1/N_{f,1}$ and $n_2/N_{f,2}$ and have numerical values of 0.25 and 0.24. Since these ratios are equivalent to $N_{o,1}/N_{f,1}$ and $\Delta N_2/N_{f,2}$ as shown in figure 1, the values of $N_{o,1}$, ΔN_1 and $N_{o,2}$ and ΔN_2 were calculated to be 320, 960, 185 000 and 59 000 cycles respectively. These values were then plotted at their corresponding stresses as shown in figure 11 and were connected by curves which approximate the shape of the original fatigue curve. These curves may then be used in separate linear summations for phase I and phase II of the fatigue process.

As a numerical example of the method of applying the double linear damage rule using these phase I and phase II curves consider a three stress level test in which the highest and lowest stresses are 290 000 and 120 000 psi.

It is required to predict the remaining life at a third stress level, 200,000 psi, after 200 and 40,000 cycles respectively have been applied at the highest and lowest stresses. Values of $N_{o,3}$ and ΔN_3 can be obtained from the phase I and phase II curves of figure 11. Thus, $N_{o,3}$ equals 5900 and ΔN_3 equals 6100. The application of 200 cycles at stress 1 results in a ratio of

$$n_1/N_{o,1} = 0.63 < 1$$

indicating that phase I has not been completed and that it is continued at the second stress level. The application of 40 000 cycles at the second stress results in a ratio of

$$\frac{n_2}{N_{o,2}} = 0.21$$

Summing up the cycle ratios applied at stresses 1 and 2 results in

$$\frac{n_1}{N_{o,1}} + \frac{n_2}{N_{o,2}} = 0.63 + 0.21 = 0.84 < 1$$

The portion, x, of the number of cycles applied at stress 3 needed to complete phase I is from equation (3),

$$\frac{x}{N_{o,3}} = 1 - \left(\frac{n_1}{N_{o,1}} + \frac{n_2}{N_{o,2}}\right)$$

$$\text{or} \quad x = 885 \text{ cycles}$$

The portion of the number of cycles applied at stress 2, needed to complete phase II is, from equation (4),

$$\frac{y}{6100} = 1 \quad \text{or} \quad y = 6100 \text{ cycles}$$

Then, the total number of cycles remaining at the third stress level is equal to

$$x + y = 885 + 6100 = 6985 \text{ cycles.}$$

APPENDIX C. - APPLICATION OF DOUBLE LINEAR DAMAGE RULE TO ALTERNATING TWO STRESS LEVEL TEST IN WHICH EXPERIMENTAL DATA ARE USED TO DEFINE PHASE I AND PHASE II OF FATIGUE PROCESS

Alternating two stress level tests were conducted as follows: First, two stress level tests were conducted at various cycle ratios, $n_1/N_{f,1}$ at a high stress, 190 000 psi, and the remaining cyclic life ratios $n_2/N_{f,2}$ were determined at a second stress, 110 000 psi. At 190 000 psi, $N_{f,1}$ was found to be 8000 cycles. At 110 000 psi, $N_{f,2}$ was found to be 625 000 cycles. These N_f values were obtained with specimens from a different heat of maraged 300 CVM steel than the data previously described in this paper for this material. The results of the tests in which different cycle ratios were applied at 190 000 psi were plotted as shown in figure 14. Best visual fit straight lines were drawn through the data, again meeting the requirement that they originate from a value of cycle ratio of 1.0 on the ordinate and abscissa. From the coordinates of the intersection point B, and the values of $N_{f,1}$ and $N_{f,2}$, the phase I and phase II parameters were determined. Thus, $N_{o,1}$ equaled 1300 cycles, ΔN_1 6700 cycles, $N_{o,2}$ 537 000 cycles, and ΔN_2 88 000 cycles. Several alternating two stress level block tests were than specified such that various fractions of 1300 cycles were applied at the high stress of 190 000 psi and identical fractions of 88 000 cycles were applied at the low stress.

The following numerical example illustrates the manner of applying the double linear damage rule to an alternating two stress level test. The example considers the case of an alternating block test in which the alternating or repeated block is taken to be one half of the number of cycles at each stress level in the base block. Both the base block and the alternating block example are shown diagrammatically in figure 15. The base block for this example (as well as all tests of figure 12) is defined as consisting of 1300 cycles at the first stress and 88 000 cycles at the second stress. To determine the number of cycles to complete phase I apply equation (3). Since

$$\frac{650}{1300} + \frac{44,000}{537,000} < 1$$

it is apparent that phase I has not been completed in the first loading block. To determine if phase I is completed in the high stress portion of the second loading block, again apply equation (3)

$$\frac{650}{1300} + \frac{44,000}{537,000} + \frac{x}{1300} = 1$$

or $x = 543$ cycles. Phase I has then been completed. Next, determine the number of cycles needed to complete phase II. Apply equation (4) to determine first whether phase II is completed in the second loading block. This gives

$$\frac{650 - 543}{6700} + \frac{44,000}{88,000} < 1$$

indicating that phase II has not been completed in block 2. Therefore, determine if phase II is completed in the high stress portion of block 3. Thus

$$\frac{650 - 543}{6700} + \frac{44,000}{88,000} + \frac{y}{6700} = 1$$

and

$$y = 3460$$

Since $y > 650$ phase II has not been completed in the high stress portion of block 3 and the next step is to determine if it is completed in the low stress portion of this block. Thus

$$\frac{650 - 543}{6700} + \frac{44,000}{88,000} + \frac{650}{6700} + \frac{z}{88,000} = 1$$

and $z = 34\ 000$. Since $z < 44\ 000$ cycles, phase II has been completed and failure occurs during the low stress portion of block 3. The total summation of cycle ratios $\frac{n}{N_f}$ for this example then is

$$\frac{n}{N_f} = \frac{650}{8000} + \frac{44{,}000}{625{,}000} + \frac{650}{8000} + \frac{44{,}000}{625{,}000} + \frac{650}{8000} + \frac{34{,}000}{625{,}000} = 0.44$$

In the same manner other apportionments of the cycles sustained at the intersection point of a two stress-level test (analogous to point B of figure 1) can be computed and the expected number of cycles to failure predicted for alternating block loading applications.

REFERENCES

1. Kaechele, L.: Review and Analysis of Cumulative-Fatigue-Damage Theories. Memorandum RM-3650-PR, Rand Corp., Aug. 1963.

2. Richart, F. E., and Newmark, N. M.: An Hypothesis for the Determination of Cumulative Damage in Fatigue, Proceedings, Am. Soc. Testing Mats., vol. 48, pp. 767-800 (1948).

3. Marco, S. M., and Starkey, W. L.: A Concept of Fatigue Damage. Trans., Am. Soc. Mech. Engrs., vol 76, pp. 627-632 (1954).

4. Corten, H. T., and Dolan, T. J.: Cumulative Fatigue Damage. Paper No. 2 of Session 3, from International Conference on Fatigue of Metals, vol. 1, Inst. of Mech. Engrs. (1956).

5. Freudenthal, A. M., and Heller, R. A.: On Stress Interaction in Fatigue and a Cumulative Damage Rule. Part I, 2024 Aluminum and SAE 4340 Steel Alloys, Wright Air Development Center, TR 58-69, AD No. 155687, June (1958).

6. Palmgren: die Lebensdauer von Kugellagern. ZVDI, vol. 68, pp. 339-341, (1924).

7. Miner, M. A.: Cumulative Damage in Fatigue. J. of Appl. Mech., vol. 12, pp. A159-A164 (1945).

8. Henry, D. L.: A Theory of Fatigue Damage in Steel. Trans. Amer. Soc. Mech. Engrs., vol. 77, pp. 913-918 (1955).

9. Manson, S. S., Nachtigall, A. J., and Freche, J. C.: A Proposed New Relation for Cumulative Fatigue Damage in Bending. Proc. Amr. Soc. Testing Materials, vol. 61, pp. 679-703 (1961).

10. Manson, S. S., Nachtigall, A. J., Ensign, C. R., and Freche, J. C.: Further Investigation of a Relation for Cumulative Fatigue Damage in Bending. ASME Trans., J. of Engr. for Ind., Feb. 1965.

11. Rally, F. C., and Sinclair, G. M.: Influence of Strain Aging on the Shape of the S-N Diagram. Rep. No. 87, Dept. of Theoretical and Appl. Mechanics, U. of Illinois, June 1955.

12. Grover, Horace J.: An Observation Concerning the Cycle Ratio in Cumulative Damage. Symposium on Fatigue of Aircraft Structures. Spec. Tech. Publ. No. 274, ASTM, pp. 120-124, 1960.

13. Manson, S. S.: Interfaces between Fatigue, Creep, and Fracture. Proc. of the International Conference on Fracture, Sendai, Japan, Sept. 14, 1965, and International Journal of Fracture Mechanics, March 1966.

14. Manson, S. S., and Hirschberg, M. H.: Prediction of Fatigue of Notched Specimens by Consideration of Crack Initiation and Propagation. Proposed NASA Technical Note.

15. Smith, R. W., Hirschberg, M. H., and Manson, S. S.: Fatigue Behavior of Materials Under Strain Cycling in Low and Intermediate Life Range. NASA TN D-1574, 1963.

TABLE I. - MATERIAL DESCRIPTION

Material	Nominal Composition	Condition	Hardness
4130 (soft)	C 0.30, Mn 0.50, P 0.040, S 0.040, Si 0.28, Cr 0.95, Mo 0.20, Fe remainder	1700° F, 1/2 hr in salt, W.Q.; 1200° F, 1/2 hr in salt, A.C.	R_c 25-27
4130 (hard)	Same as above	1600° F, 1/2 hr in salt, W.Q; 750° F, 1 hr in salt, A.C.	R_c 39-40
300 CVM	C 0.03 max, Si 0.10 max, Mn 0.10 max, S 0.010 max, P 0.010 max, Ni 18.50, Co 9.00, Mo 4.80, Al 0.10, Ti 0.60, B 0.003, Zr 0.02 added Ca 0.05 added	900° F, $3\frac{1}{2}$ hr, A.C.	R_c 52

TABLE II. - MECHANICAL PROPERTIES OF TEST MATERIALS

Material	Y.S. 0.2 percent offset, ksi	UTS, ksi	Fracture strength, ksi	R.A., percent	Mod. of elas., psi
4130 (soft)	113	130	245	67.3	32×10^6
4130 (hard)	197	207	302	54.7	29
300 CVM	-	295	380	50.7	27

E-3558

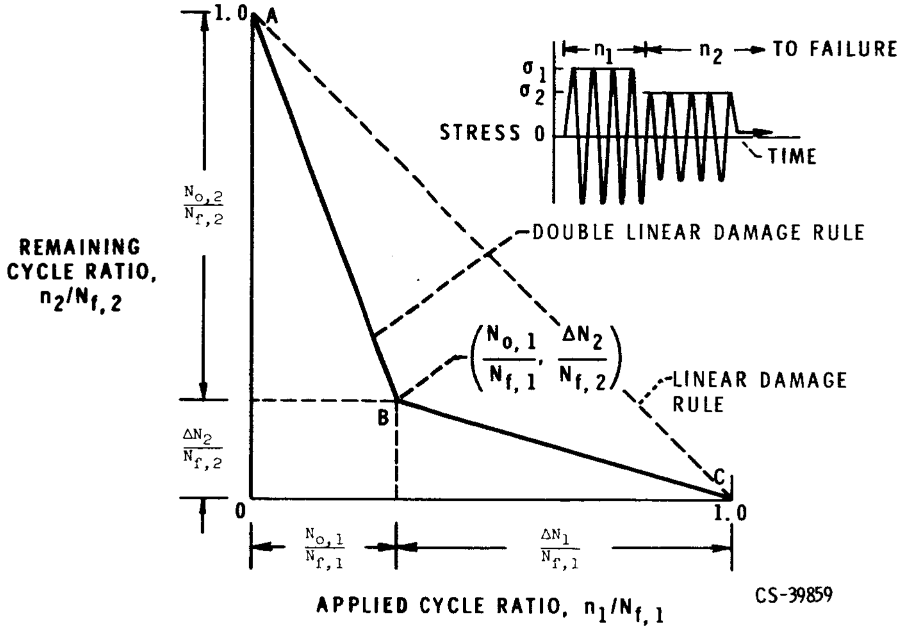

Fig. 1. - Fatigue damage in two stress level tests interpreted by linear damage rules.

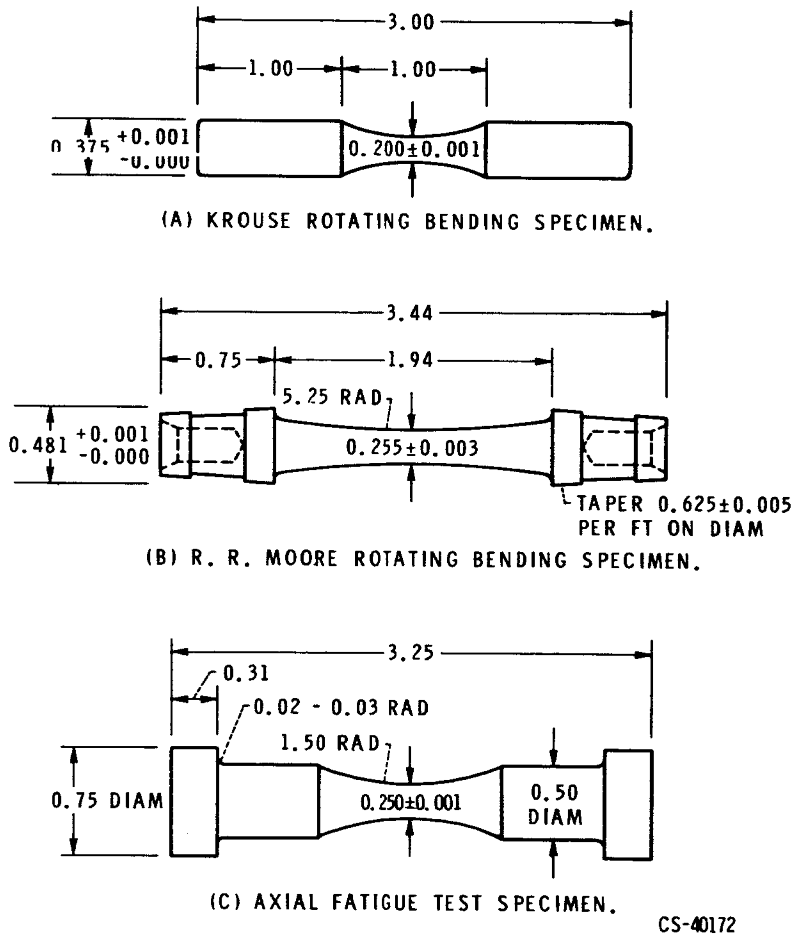

Fig. 2. - Fatigue specimens.

E-3558

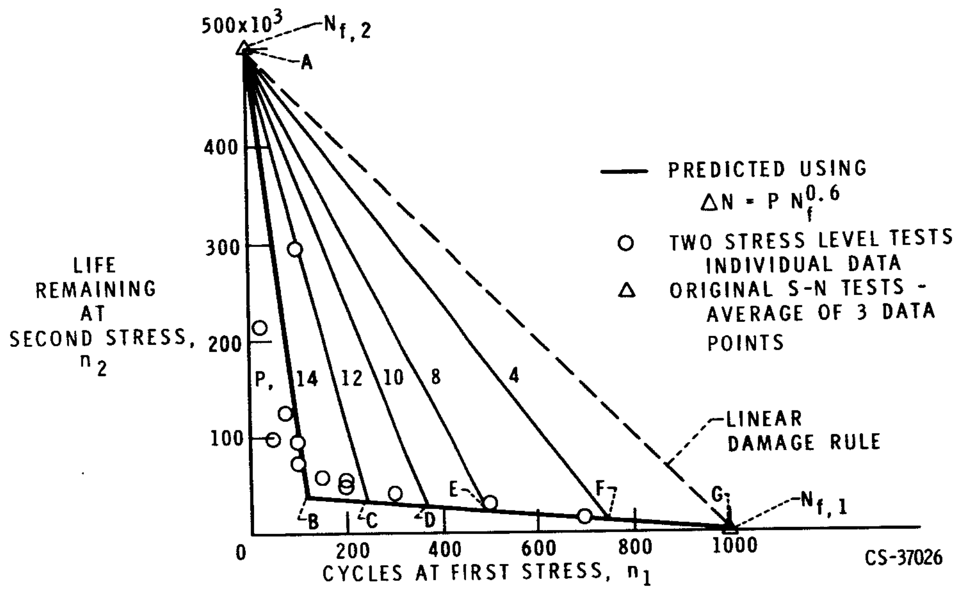

Fig. 3. - Two stress level rotating bending fatigue tests for determination of coefficient in expression for crack propagation. Material, maraged 300 CVM steel.

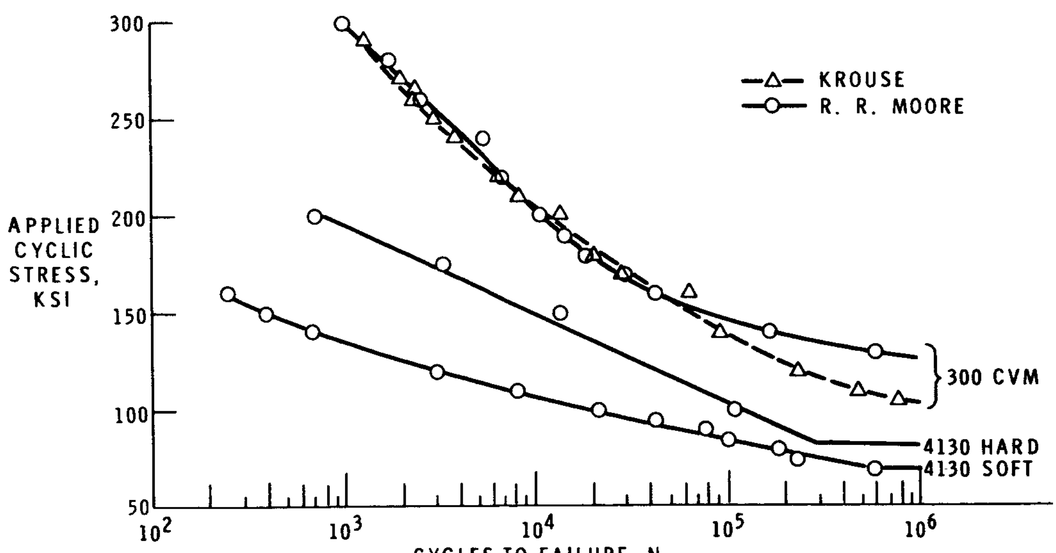

(a) Rotating bending.

Fig. 4. - Fatigue curves for materials investigated.

E-3558

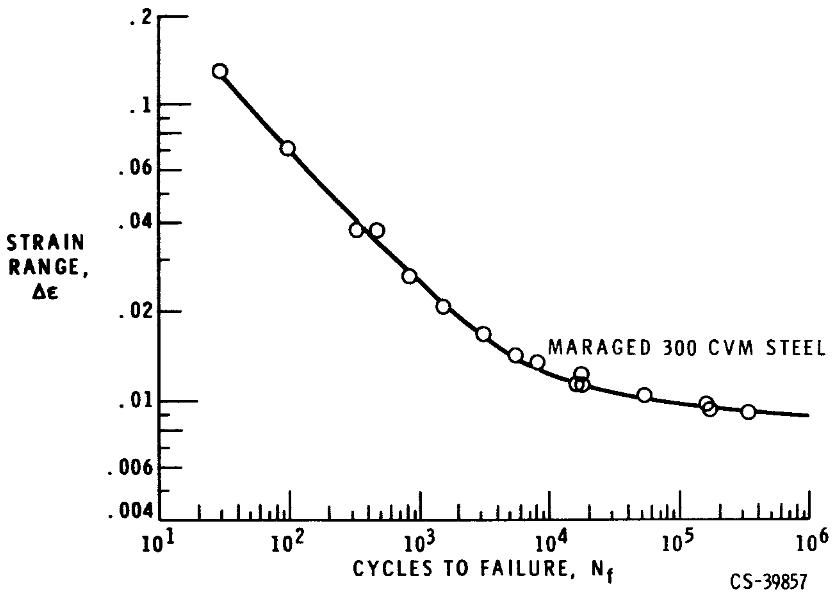

(b) Axial strain cycling.

Fig. 4. - Concluded.

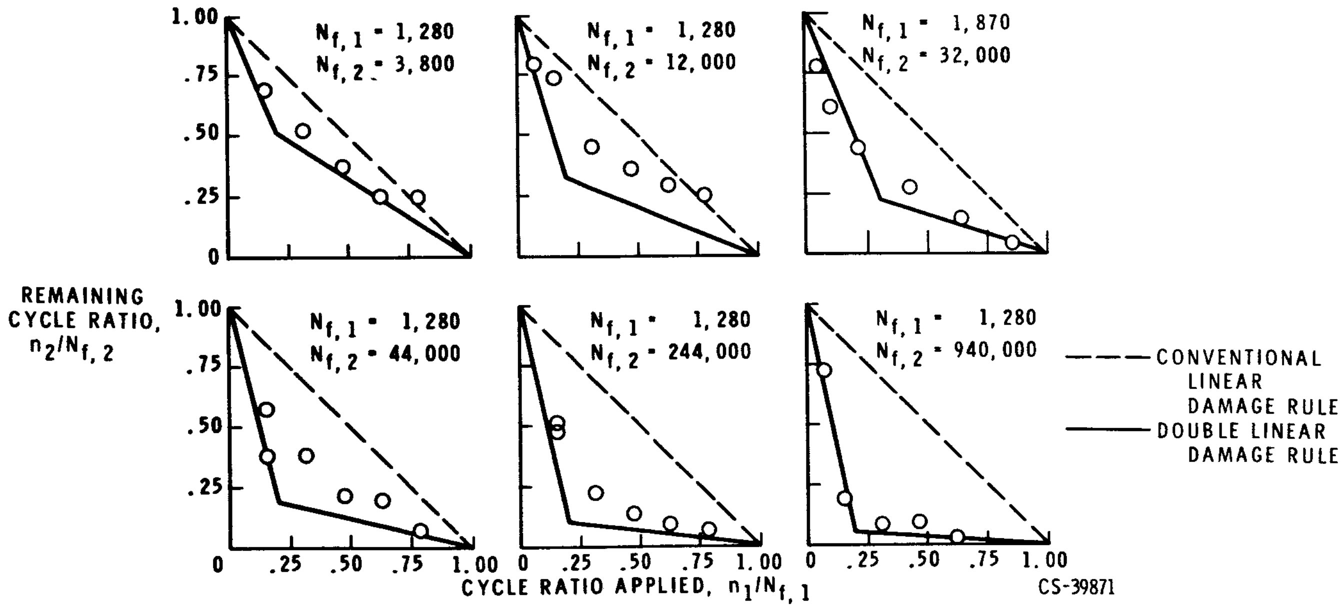

(a) Krouse rotating bending - high to low stress with low initial life.

Fig. 5. - Comparison of predicted fatigue behavior by conventional and double linear damage rules with experimental data for two stress (strain) level tests. Material, maraged 300 CVM steel.

E-3553

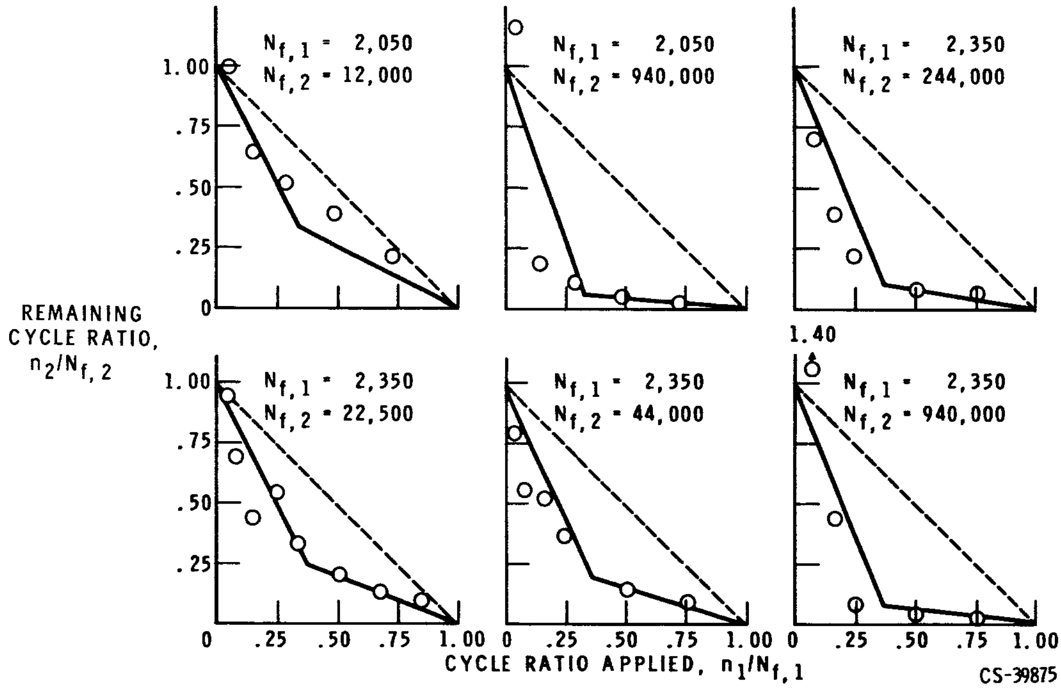

Fig. 5(a). - Continued.

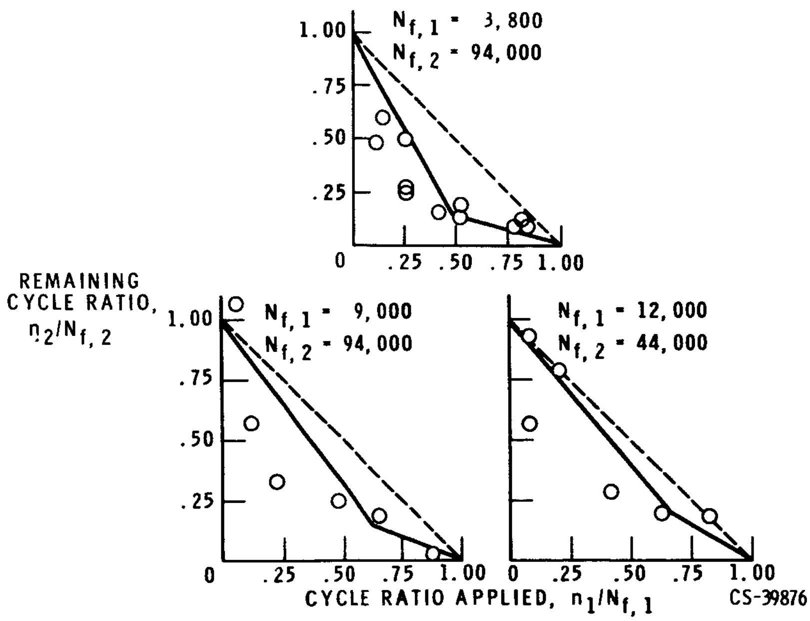

(b) Krouse rotating bending - high to low stress with high initial life.

Fig. 5. - Continued.

E-3558

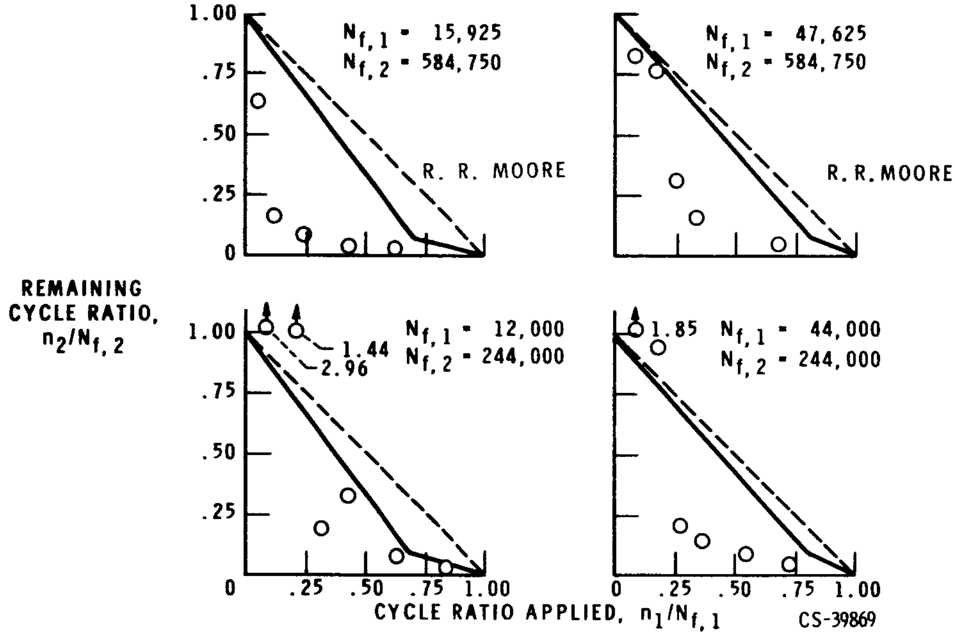

Fig. 5(b). - Continued.

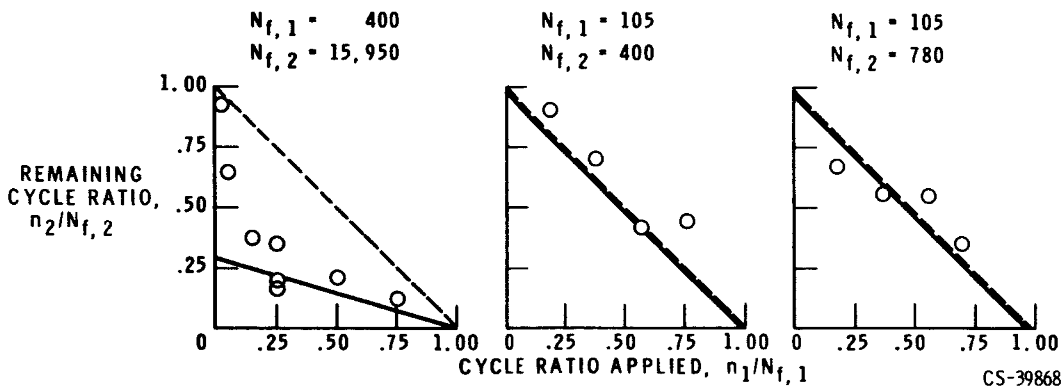

(c) Axial strain cycling - high to low strain with low initial life.

Fig. 5. - Continued.

E-3558

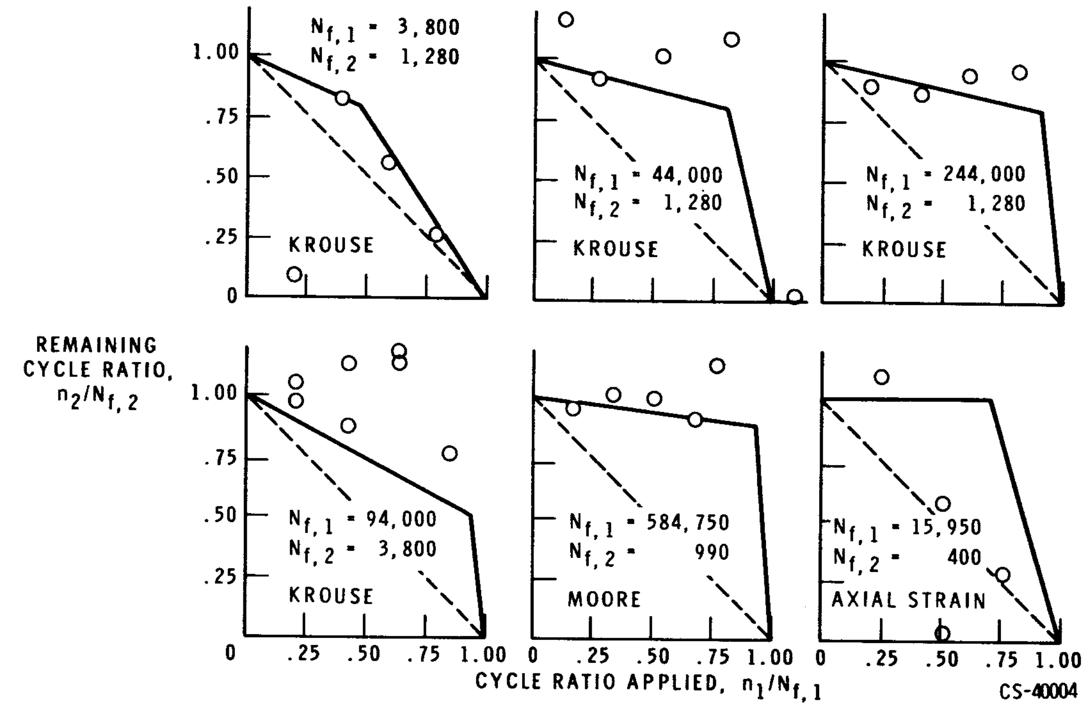

(d) Rotating bending and axial strain cycling - low to high stress (strain).

Figure 5. - Concluded.

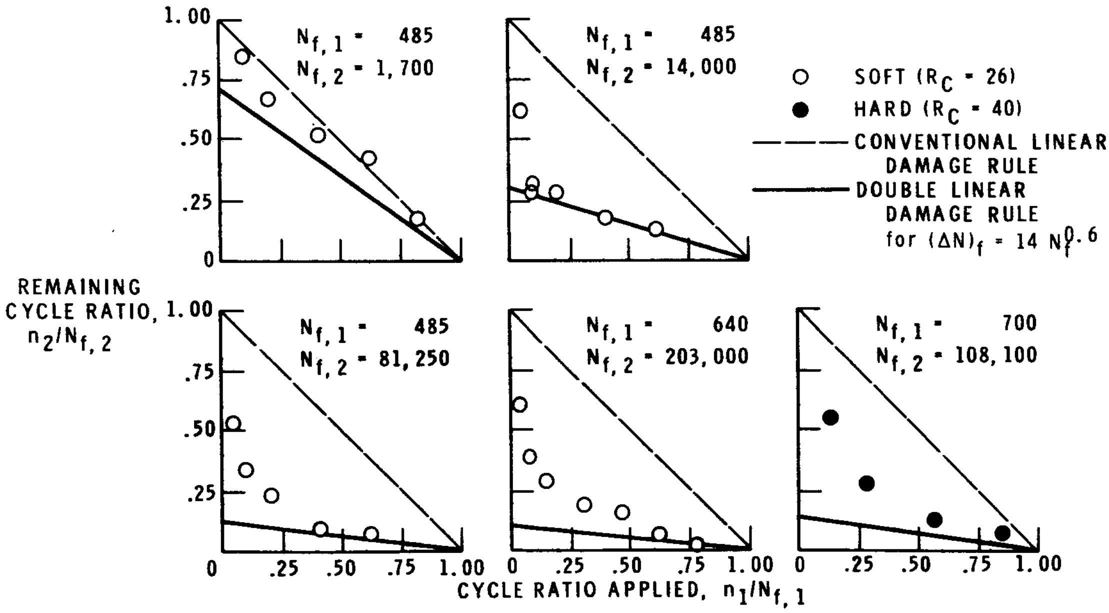

(a) R. R. Moore rotating bending - high to low stress with low initial life.

Fig. 6. - Comparison of predicted fatigue behavior by conventional and double linear damage rules with experimental data for two stress level tests. Material, SAE 4130 steel.

E-3558

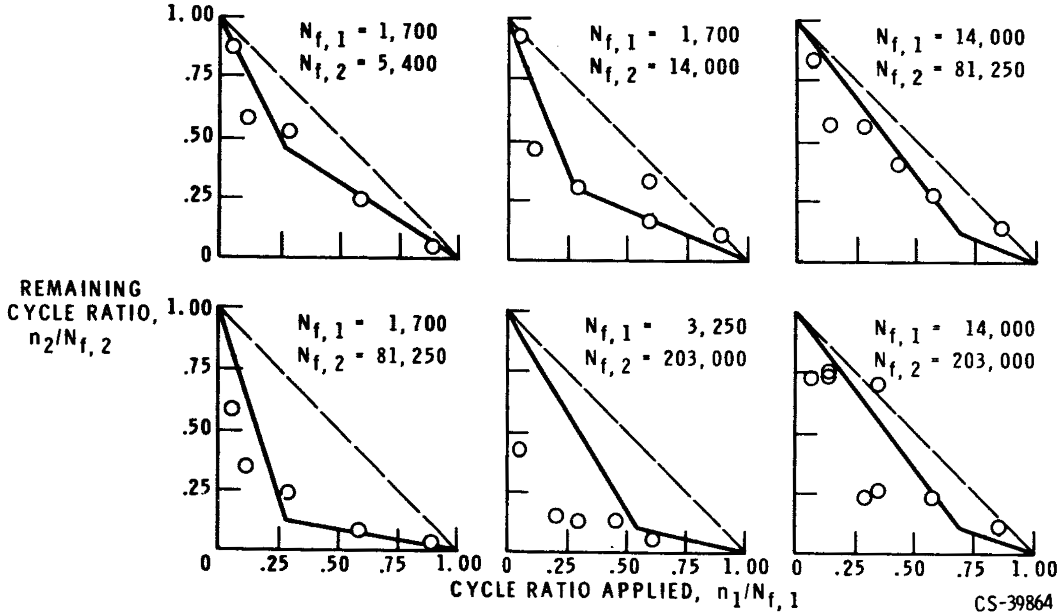

(b) R. R. Moore rotating bending - high to low stress with relatively high initial life.

Fig. 6. - Concluded.

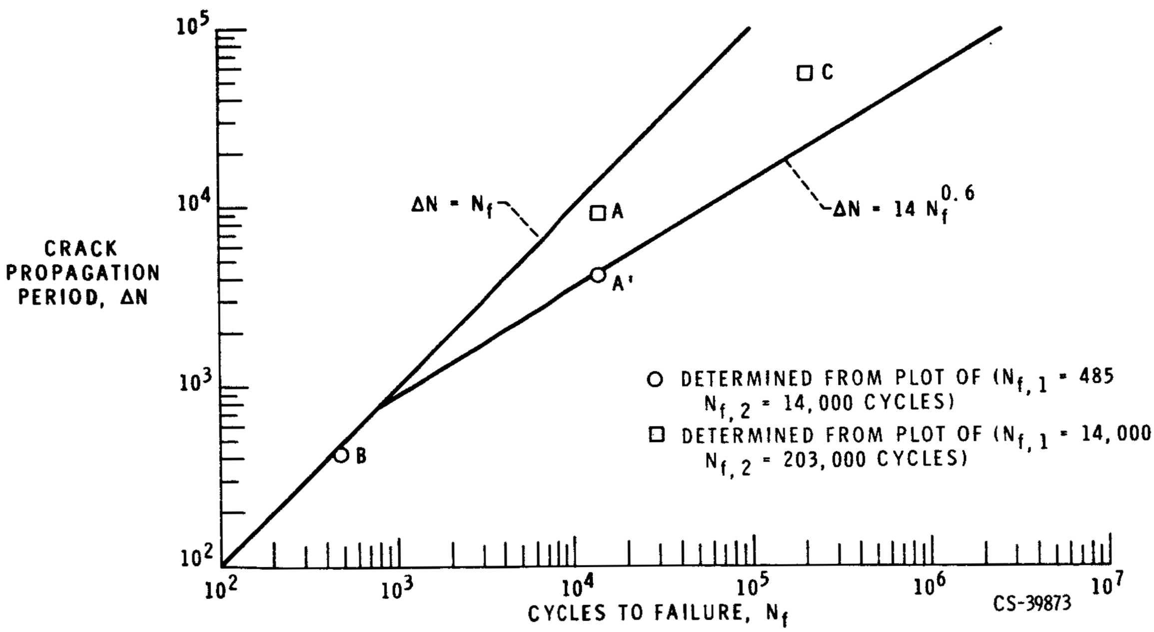

Fig. 7. - Effect of stress combinations in determination of crack propagation period. Material, 4130 soft steel, R. R. Moore rotating bending tests.

E-3558

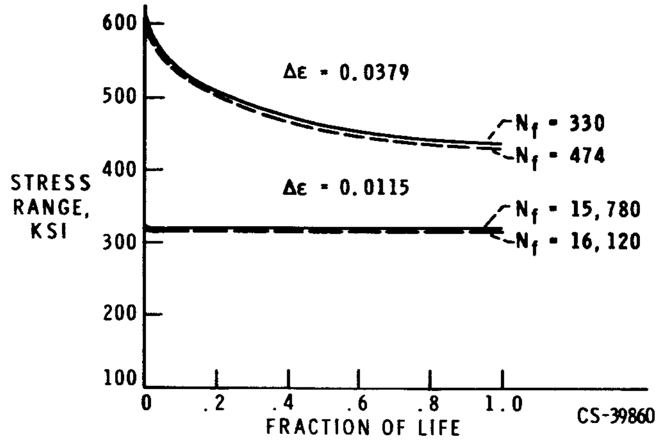

Fig. 8. - Stress response in axial strain cycling for constant strain amplitude tests of maraged 300 CVM steel.

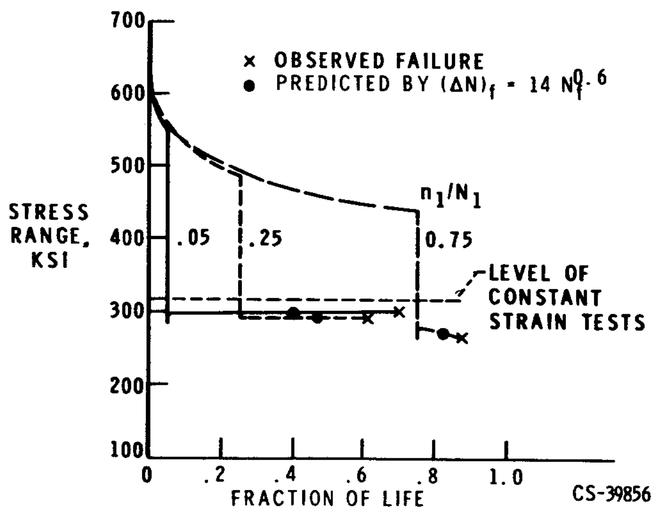

Fig. 9. - Stress response in axial strain cycling two strain level tests of maraged 300 CVM steel.

E-3558

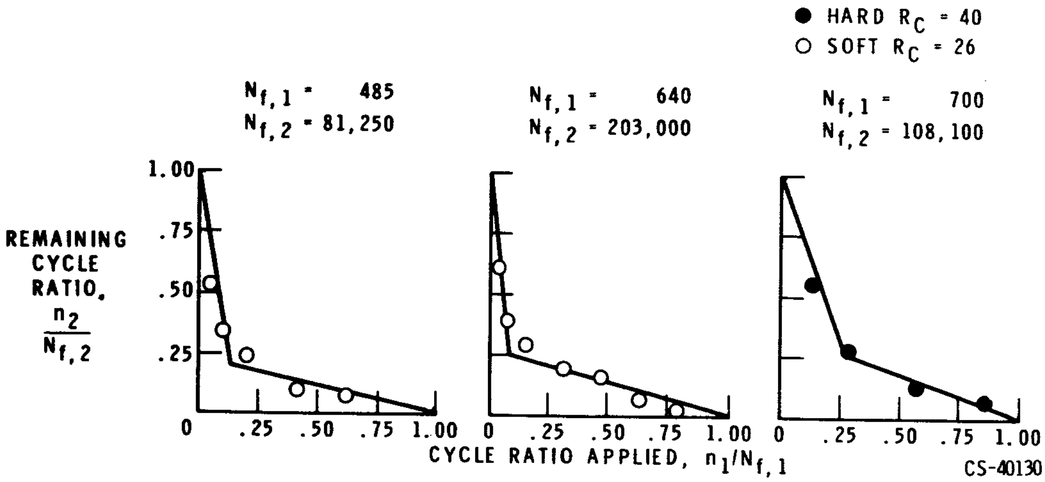

Fig. 10. - Illustration of fit of two straight lines to rotating bending data obtained from two stress level tests with SAE 4130 steel.

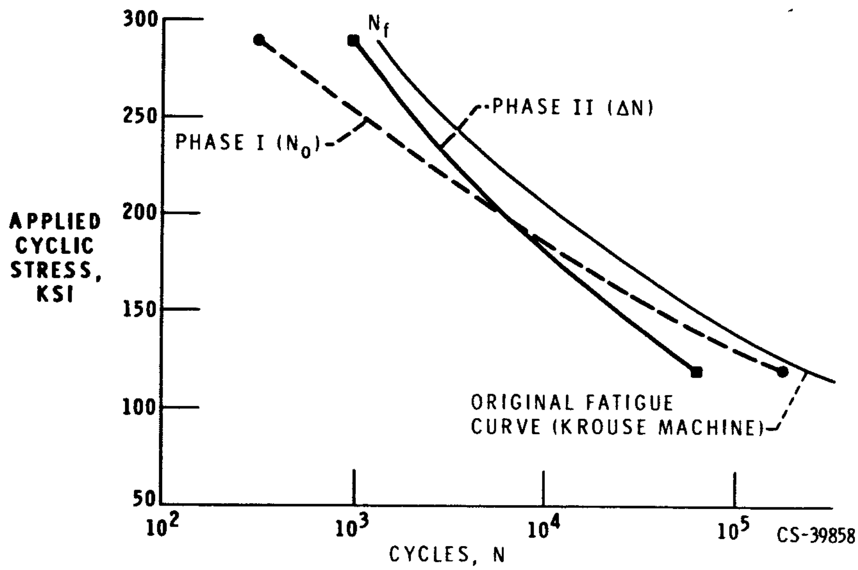

Fig. 11. - Determination of phase I and phase II of fatigue process from two-stress level tests at highest and lowest stress levels of loading spectrum. Material, maraged 300 CVM steel.

E-3558

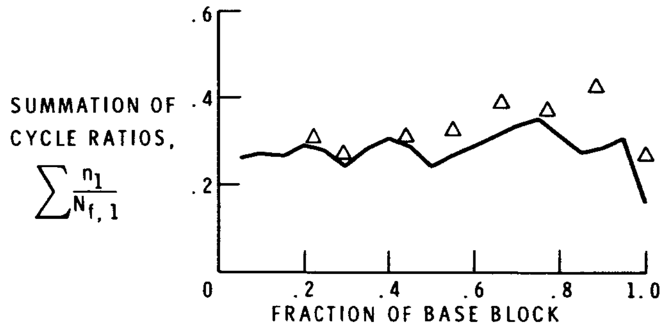

(a) Summation of cycle ratios applied at high stress.

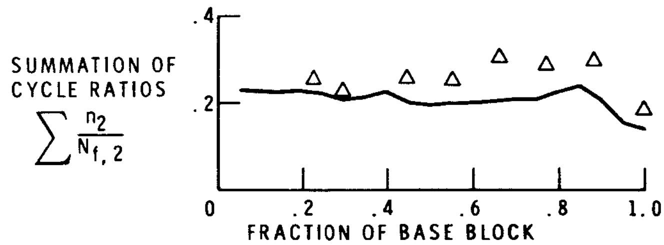

(b) Summation of cycle ratios applied at low stress.

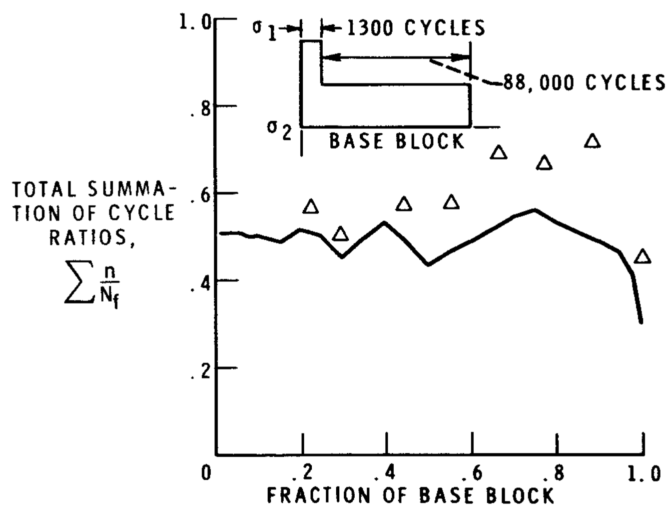

(c) Total summation of cycle ratios.

Figure 12. - Comparison of experimental and predicted summation of cycle ratios for alternating two stress level tests. Predictions made by double linear damage rule using experimental data to define Phase I and Phase II fatigue process.

E-3558

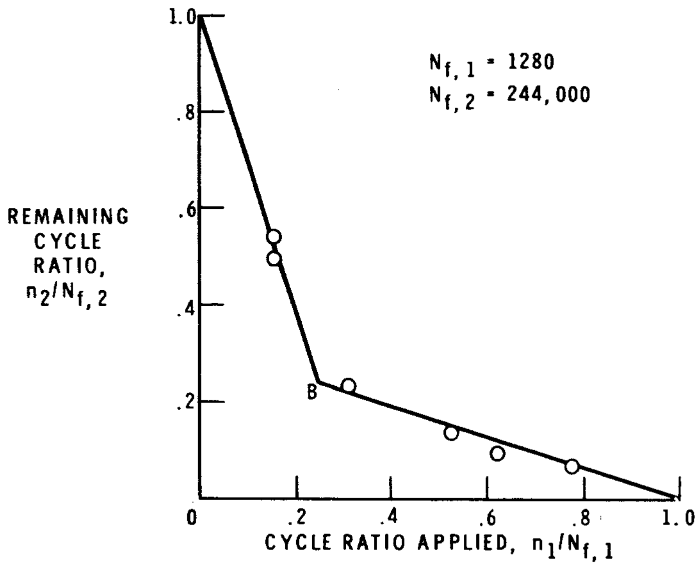

Fig. 13. - Two straight lines fitted to data from two stress level tests of maraged 300 CVM steel.

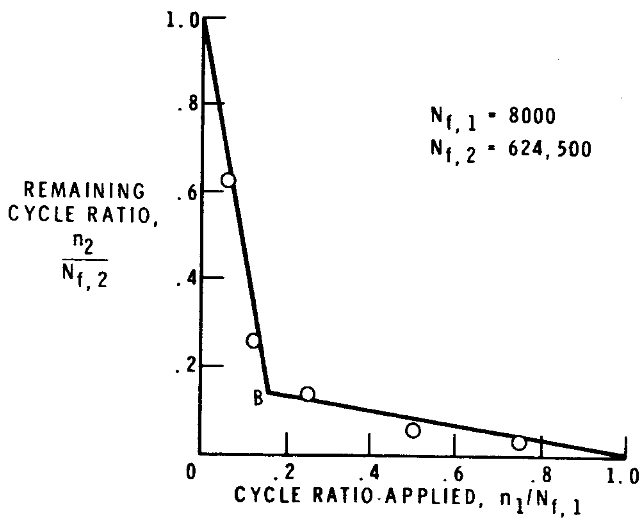

Fig. 14. - Experimental determination of Phase I and Phase II transition used in conjunction with double linear damage rule. Material, maraged 300 CVM steel.

E-3558

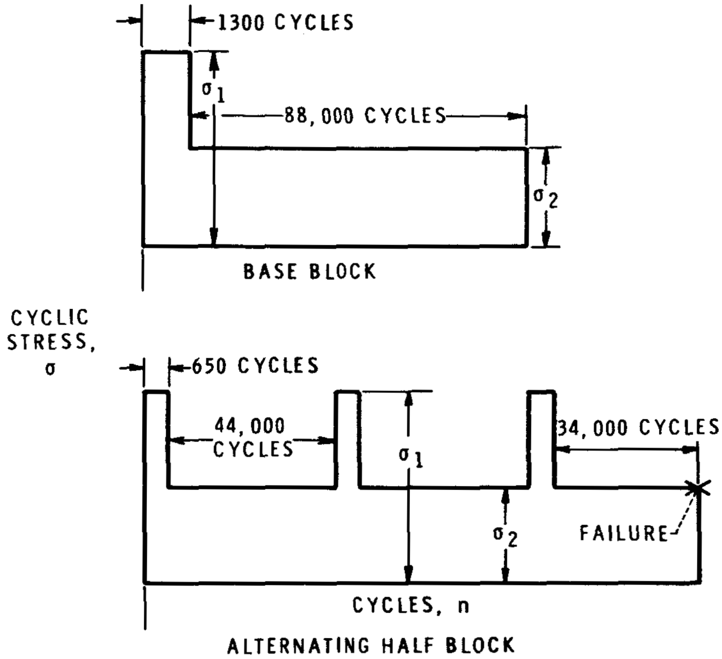

Fig. 15. - Diagram of loading pattern for numerical example of appendix c.